INVESTIGATING THE IMPACT OF IN-VEHICLE TRANSIENTS ON DIESEL SOOT EMISSIONS

by

Zoran FILIPI, Jonathan HAGENA, and Hosam FATHY

This paper describes development of a test cell setup for concurrent running of a real engine and a simulation of the vehicle system, and its use for investigating highly-dynamic engine-in-vehicle operation and its effect on diesel engine emissions. Running an engine in the test cell under conditions experienced in the vehicle enables acquiring detailed insight into dynamic interactions between powertrain sub-systems, and the impact of it on fuel consumption and transient emissions. This type of data may otherwise be difficult and extremely costly to obtain from a vehicle prototype test. In particular, engine system response during critical transients and the effect of transient excursions on emissions are investigated using advanced, fast-response test instrumentation and emissions analyzers. Main enablers of the work include the highly dynamic AC electric dynamometer with the accompanying computerized control system and the computationally efficient simulation of the driveline/vehicle system. The latter is developed through systematic energy-based proper modeling that tailors the virtual model to capture critical powertrain transients while running in real time. Coupling the real engine with the virtual driveline/vehicle offers a chance to easily modify vehicle parameters, and even study different powertrain configurations. In particular, the paper describes the engine-in-the-loop study of a V-8, 6l engine coupled to a virtual 4 4 off road vehicle. This engine is considered as a high-performance option for this truck and the real prototype of the complete vehicle does not exist yet. The results shed light on critical transients in a conventional powertrain and their effect on NO$_x$ and soot emissions. Measurements demonstrate very large spikes of particulate concentration at the initiation of vehicle acceleration events. Characterization of transients and their effect on particulate emission provides a basis for devising engine-level or vehicle level strategies, and direct guidance for developing drive-by-wire systems and/or hybrid supervisory control.

Key words: *diesel engine, soot emissions, transients, engine-in-the-loop*

Introduction

Diesel engines are particularly well suited for medium-duty vehicles due to their superior fuel economy, favourable torque and power ratings, and durability. Recent technological advances, particularly related to fuel injection and air-charging systems, have led to increased performance and refinement. Hence, diesels are becoming an attractive option for light trucks as well. However, additional design improvements are necessary for diesel propulsion systems to address the rapid rise of fuel prices and the tighter emissions standards announced by the US En-

vironmental Protection Agency (EPA) and its European Union counterpart for the time frame 2007-2010. Dual-use and off-road diesel-powered trucks must meet aggressive fuel economy and emissions requirements under harsher missions. In addition, soot emission is related to visual signature and loading of aftertreatment components that will likely be necessary in near future.

Developing a modern propulsion system invariably entails some degree of prototyping. Simulation tools are indispensable for the rapid prediction of vehicle behaviour during a typical mission and the evaluation and selection of propulsion concepts and components early in the design process [1-9]. Simulation tools also make it possible to vary and optimize component and sub-system designs for given goals and constraints [10, 11]. However, simulation-based vehicle system design is not without limitations. Conducting vehicle-level studies over complete driving schedules limits the degree of fidelity that can be afforded within a reasonable computational time frame. For instance, simulating soot formation processes in a diesel engine is prohibitively slow in the context of systems work, since it requires coupling of sophisticated computational fluid dynamics (CFD) models and chemical kinetics [12, 13]. Therefore, even though state-of-the-art vehicle simulations enable assessing vehicle performance, fuel economy and dynamic response with high confidence, verification of emissions trends necessitates experimentation. Merging the virtual and real worlds, by combining physical engines with virtual drivelines and vehicles, is perhaps the only way to accurately characterize the influence of system design on performance, fuel economy, and emissions early in the design cycle.

This paper couples the virtual simulation and real experimentation, and introduces a setup that concurrently runs a driveline/vehicle simulation and a real engine in a test cell. In contrast with more traditional implementation of the hardware-in-the-loop (HIL) that typically features a control unit in hardware integrated with virtual devices and systems being controlled, a major piece of hardware is integrated with virtual devices emulating realistic operating conditions. Using the virtual driveline/vehicle simulation enables rapid prototyping and optimization of different powertrain configurations, designs, and control systems. Furthermore, by implementing the complete engine system in physical hardware, the setup captures the effect of uncertainties in actuator response on engine dynamic behavior. Consequently, our use of HIL simulation is not limited to control design, testing and calibration, but addresses broader objectives of evaluating an integrated powertrain system configuration, system optimization, and power management design. Secondly, the setup immerses a major piece of hardware, namely, a multi-cylinder diesel engine together with its accompanying sub-system controller, in the loop and that motivates the use of the term engine-in-the-loop (EIL) simulation.

Engine- (or powertrain-) in-the-loop testing is frequently used in industry, but mostly for the design and calibration of transmission and engine controllers [14]. Jason and Moskwa [15], for instance, describe the enhancement of dynamometer bandwidths using the hydrostatic principle for the purpose of system control and diagnostics. Similarly, Fleming *et al.* [16] describe the development of a powertrain-in-the-loop setup that enables control design specifically for parallel hybrid electric vehicles. Finally, the Argonne National Laboratory (ANL) serves as the primary site for technology validation for the U. S. Department of Energy. Their focus is on enabling the testing of various components in an emulated vehicle environment [10]. Recent work at the ANL has also utilized HIL simulation to investigate tradeoffs between fuel efficiency and NO_x emissions in a hybrid vehicle with a continuously variable transmission (CVT) [17], but relied primarily on analysis of the time spent at given engine regimes and steady-state emission maps. Our focus differs from the above EIL-related literature in three ways. First, we explore the capabilities of EIL as a research tool for studying fundamental aspects of transient diesel emissions in the context of realistic in-vehicle conditions. We seek a

characterization of powertrain dynamics, and a fundamental understanding of the influence of such transient dynamics on engine exhaust emissions. Secondly, we support the use of EIL as an integrated system-level methodology for powertrain design and control with extensive driveline/vehicle modeling effort. Prior research in the Automotive Research Center at the University of Michigan (ARC) produced a comprehensive set of simulation tools for design and analysis of advanced vehicle systems that provide a strong foundation for development of real-time models. The system modeling platform dubbed VESIM for vehicle engine simulation has been developed in Simulink with emphasis on high-fidelity of fully integrated system simulations. The tool can be configured for different propulsion system architectures, such as the conventional vehicle [2] or different hybrid options [3, 6]. Thirdly, our focus is on medium-duty diesel engines and trucks, rather than passenger cars. The engine used in this work is a 6 L V-8 diesel produced by the International Truck and Engine Corporation (International), and it is coupled to a highly dynamic AC dynamometer in the W. E. Lay Automotive Laboratory at the University of Michigan. The virtual vehicle is configured based on the specifications of the high mobility multipurpose wheeled vehicle (HMMWV or a Hummer), a 4 4 vehicle with exceptional off-road capabilities.

The objectives of the work are to develop the EIL experimentation capability and use it to study engine system behavior when coupled to a 4 4 driveline with a four-speed automatic transmission (fig. 1). In particular, we examine and characterize transient emissions of NO_x and particulates and assess the impact of transient spikes on overall emissions. Studying the dynamic interactions between different vehicle sub-systems sheds light on causes for critical transient conditions and suggests potential engine-level or vehicle-level approaches for active transient emission reduction. As an example, the hypothesis that the increased presence of internal residual during turbo

Figure 1. A schematic of the 4 4 powertrain for the off-road truck
Engine and ICM – injection control module, T/C – torque converter, Trans – transmission, Tr case – transfer case, D-F and D-R – front and rear differential, respectively

lag has a strong effect on increased particulate formation is explored, hence offering guidance for optimization of the air and exhaust gas recirculation (EGR) systems. The tradeoff between the torque response and the magnitude of the transient soot spike is assessed by analyzing a load-increase event with three tip-in functions, *i. e.* a step change, a two-second, and a five-second tip-in. This generates detailed guidance for development of future drive-by-wire strategies or hybrid vehicle power management strategies optimized for clean and efficient operation.

The paper begins with a high-level description of the approach, critical enablers, and EIL setup used in this work. Next, modeling and integration challenges are described briefly. This is followed by a detailed description of diesel engine specifications, test cell instrumentation and the interface between the dynamometer and the vehicle simulation. The setup's V-8 6L diesel engine manufactured by International is a new product, much more powerful than the standard Hummer engine, and it is being considered for propulsion of heavier versions of the vehicle. The use of the setup for quantifying the influence of powertrain transients on dynamic die-
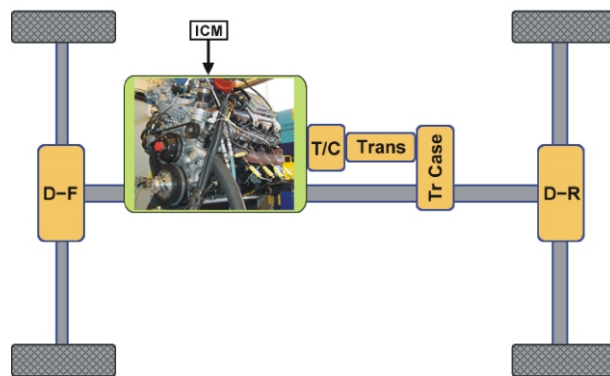
sel engine performance and emissions is demonstrated through analysis of drive cycle results. Particular attention is given to analysis of transient soot emission spikes observed at every rapid load increase. The investigation of in-vehicle transients is complemented with in-depth analysis of engine parameters obtained for different tip-in functions. Full characterization of transient particulate emission produces guidelines for developing future clean and efficient drive-by-wire or hybrid power management strategies. Finally, the paper ends with a brief summary and conclusions.

Approach – inserting major piece of hardware in-the-loop

Conceptual considerations

Several key enablers are necessary before a full EIL capability can be fully developed. Figure 2 presents a conceptual summary of such enablers (in ovals) in relation to a HIL setup's main components (in rectangles).
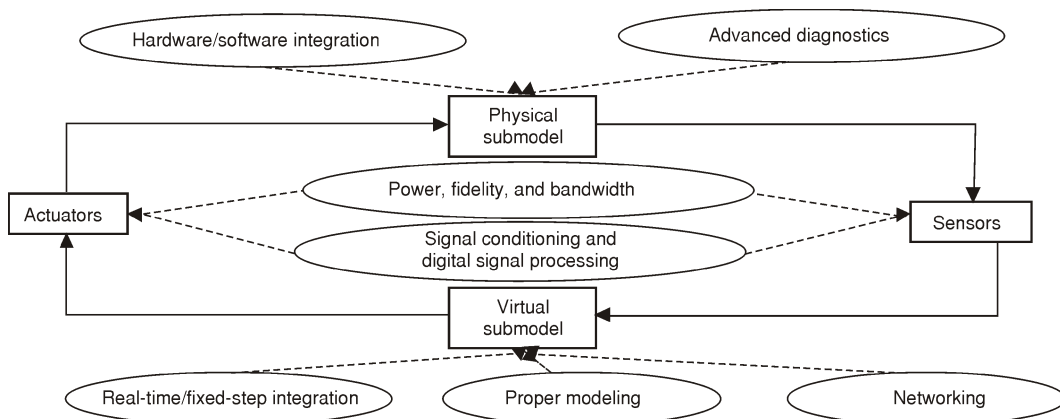

Figure 2. Key enablers of HIL simulation

The specific requirements pertaining to each one of the items in fig. 2 are dictated by the HIL application. In case of the EIL setup, the following was found to be essential:
(1) *Sensor and actuator fidelity and bandwidth, and unobtrusiveness.* The particular dynamometer furnished by AVL LIST GmbH possesses a very low inertia that minimizes its influence on perceived engine inertia, thereby minimizing obtrusiveness. Sensors used on the setup have fidelities and bandwidths sufficient for the accurate measurement and control of highly transient engine dynamics.
(2) *Signal conditioning and digital signal processing.* The setup employs finely tuned lead-lag filters to both minimize the effect of measurement noise and maximize its bandwidth. Such signal conditioning has proven critical to the integration effort and effective exploitation of the setup's capabilities.
(3) *Fast processors and fixed-step integration.* The setup uses state-of-the-art microprocessors and real-time operating systems to ensure real-time simulation. A fixed step-size integration routine within the Matlab Real-Time Workshop ensures that the simulator is constantly in synch with real time. The particular communication system used in the setup (EMCON) was designed by AVL to ensure maximum bandwidth, thereby ensuring high-fidelity HIL simulation.

(4) *Advanced diagnostics of physical devices*. Engine instrumentation includes specialized fast-response analyzers for measuring critical engine-out emissions during very dynamic events characteristic of powertrain operation in an off-road vehicle.

(5) *Proper modelling*. The setup uses proper virtual driveline and vehicle models to ensure that the dynamics of the driveline and vehicle are captured both accurately and in real time. The extraction of such models from more complex ones using energy-based model reduction techniques is described in depth in other publications by the authors [18-20].

(6) *Networking*. While this is not part of the scope of the current study, the capabilities of the setup will enable future consideration of networking HIL simulators to allow different engineering teams to design selected subsystems independently and then integrate their design efforts through the Internet.

(7) *Hardware/software integration*. The engine is prototyped in hardware and the rest of the vehicle system is virtual. This partitioning enables generating critical data experimentally (*e. g.* details of engine transient processes and emissions) and rapid prototyping of different vehicle driveline options. In particular, the setup makes it possible to quickly swap and compare different transmission options, including manual, automatic, hybrid electric or hydraulic options.

Integration of the EIL setup

The integration of the virtual components with the hardware in the test cell to create an engine-in-the-loop system is represented schematically in fig. 3. An advanced test cell, featuring a state-of-the art medium duty diesel engine and a highly dynamic AC dynamometer with the accompanying control system, has been set up for investigations of clean diesel technologies [21]. The dynamometer and test cell hardware vendor (AVL North America) committed to providing the necessary hardware and software for interfacing models in Simulink with the dynamometer and engine controller, thus opening up the possibility of realizing the full benefit of the synergy between modeling and experimental efforts. The VESIM developed in the ARC is used to simulate the vehicle's driver, driveline, hybrid components, controllers, and vehicle dynamics [2, 3, 6]. VESIM's forward-looking driveline and vehicle dynamics models make it possible to integrate a virtual driver into the system with the vehicle driving schedule as the only input to the EIL models.
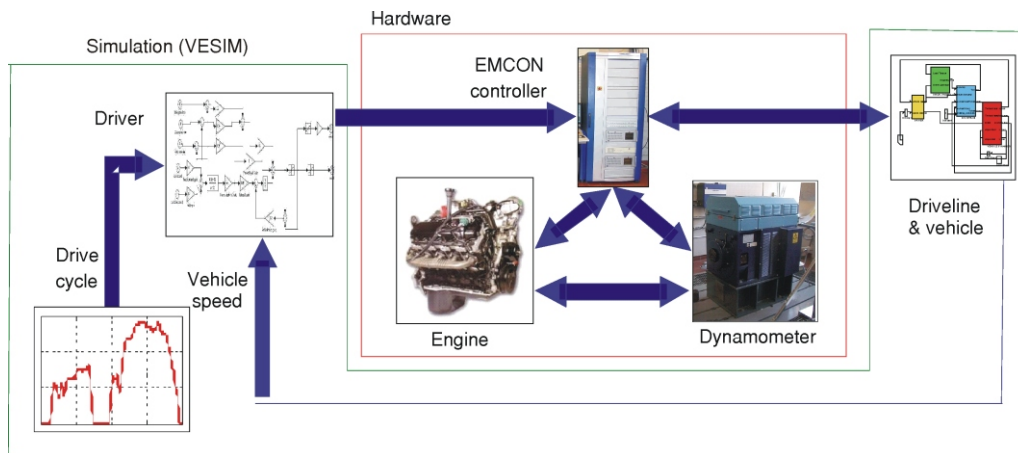

Figure 3. Engine-in-the-loop test cell configuration

The driveline and vehicle simulations run concurrently with the engine in real time to simulate vehicle behavior and provide feedback to the virtual driver and dynamometer controller (EMCON). The engine is coupled to the dynamometer and EMCON, such that its performance depends entirely on signals provided by the driver and response of the virtual vehicle. This constitutes a fully integrated EIL setup that emulates the desired vehicle, drivetrain, and driver concurrently in real time.

To illustrate the communication flow, consider a drive cycle at the beginning of which the engine is idling and the vehicle velocity is zero. As the target velocity starts to increase, the virtual driver within VESIM recognizes the difference in demanded and actual vehicle velocities and increases the accelerator pedal position appropriately. This pedal position signal is passed to EMCON and is processed into a signal that is sent to the engine. The engine responds to this signal by producing torque measured by the dynamometer. This torque value is then used as input into the VESIM driveline/vehicle module capable of calculating the impact of the supplied torque on vehicle velocity. The updated vehicle velocity is subsequently translated to engine speed, based on current states in the transmission and torque converter, and this request is sent to the dynamometer through EMCON. The updated vehicle velocity is also provided to the driver, which again compares this value to the driving schedule and determines the pedal position for the following step. When the desired vehicle velocity profile starts to fall, the virtual driver "lifts the foot off the gas pedal" thus making the gas pedal signal zero, and instead sends an appropriate command to a virtual brake model within VESIM. Vehicle velocity changes according to the brake model, and engine speed is commanded appropriately. Thus, the above setup enables the fully integrated simulation of acceleration, coasting, and braking events.

Modeling and integration challenges

Modeling is supported by the ongoing research in the ARC. The main mission of the center is development of advanced models and simulations of ground vehicles, with an emphasis on predictive fully integrated system simulations. Various subsystem models have been integrated in Simulink as a common simulation environment to produce a tool for conventional vehicle simulation dubbed VESIM [2]. This platform has subsequently been expanded and utilized for investigating a number of research issues related to advanced and hybrid truck propulsion. The fuel economy potential of selected hybrid electric and hydraulic hybrid configurations has been evaluated by Lin *et al*. in [6, 7] and Filipi *et al*. [3]. Hierarchical methodologies for optimally designing a complex vehicle system are explored in [11], while [22] considers design under uncertainty.

Successful EIL simulation requires proper driveline/vehicle models, *i. e*., models complex enough to accurately capture powertrain dynamics but simple enough to run in real time [23]. A 5112 kg HMMWV with a conventional powertrain was previously modeled using bond graphs [18]. A bond graph is a schematic that represents a given dynamic system as an assembly of energy sources, stores, and dissipaters exchanging energy and information [24, 25]. The models were then made proper by balancing their fidelity *vs*. complexity using the model order reduction algorithm (MORA) by Louca *et al*. [26]. The fundamental premise behind MORA is that an energetic element's activity is indicative of its importance to the model's fidelity. The fidelity of the developed models was verified using the accuracy and validation algorithm for simulation (AVASim) by Sendur *et al*. [20]. AVASim quantifies a model's fidelity by comparing its outputs to a benchmark, which may be either an experiment or a higher-fidelity model. Finally, a proper model of an existing Hummer is constructed in a way that captures powertrain transients accurately while being simple enough to run in real time [18, 19]. This model's pa-

rameters were then scaled to match the engine used in this case study. In particular, the Hummer torque converter, gear ratios, shift map, and final drive were scaled to provide desired mobility, smooth shifting, and fuel efficiency, given the speed and torque range of the International V-8 engine [27].

The above super-Hummer models were expressed in the bond graph language SIDOPS and implemented in the modeling tool 20Sim [28]. For EIL simulation, the engine module was removed and the drivetrain was connected to the EMCON interface. The models were then translated into differential algebraic equations (DAEs) and expressed in the C language. Embedding the C code into Simulink as a Simulink-executable S-function (using Matlab's external interface C-MEX function) finally allowed the models to be connected to the EMCON interface.

A viable EIL simulator comprises more than just well-instrumented hardware connected to proper virtual models. Initial work quickly uncovered integration issues that needed to be addressed on both ends before the setup could be operated safely and with full functionality. The main challenges proved to be:
– connection causality,
– signal noise and communication delays, and
– virtual driver response.

The most basic integration question is connection causality, namely, which signals enter each subsystem as inputs, and which are generated as outputs. Traditionally, engine-dynamometer and EIL test setups commanded engine torque and measured engine speed through a dynamometer [15,16, 29]. However, the use of this causality for EIL simulation often led to unstable engine torque signals. Controlling engine torque through a dynamometer implicitly involves engine acceleration control. Acceleration is inherently higher in order compared to velocity. Higher-order signals are noisier to measure, and their control requires higher actuator bandwidths compared to lower-order signals. A dynamometer is hence generally more effective for commanding engine speed rather than torque. In this work, reversing the EIL setup's connection causality by commanding the engine's speed and measuring its torque alleviated the stability problem and increased the setup's bandwidth to the desired range (15-25 Hz). The virtual model causality was reversed by incorporating impeller inertia into the torque converter model. More details are provided by Filipi *et al*. [21].

The second integration challenge was a result of the fact that measured signals are prone to both noise and communication time delays. These two problems were addressed through the introduction of low-pass filtering to eliminate sensor noise and lead filtering to counterbalance the phase lag introduced by the communication time delays. The lead-lag filter design procedure involved operating the engine at steady-state, and then superimposing sinusoidal engine speed and pedal position profiles onto the steady-state. Repeating this for various frequencies furnished empirical transfer functions representing the engine's dynamics and empirical models of the setup's noise. These models were then used to design the lead-lag filters through loop shaping, a widely used process whose details are omitted for brevity [30, 31].

The final integration challenge was the virtual driver's inability to follow the rapid fluctuations of vehicle speed in a city driving cycle accurately. This drive cycle is prescribed by the EPA for emissions testing. For certification purposes, the velocity profile must be followed with an error not exceeding one mile per hour for more than one second. This is relatively difficult even for real drivers, and EPA allows preview during certification tests. The driver model developed for the EIL study was initially a simple proportional-integral-derivative controler model with an anti-windup loop. Adding a low-pass filter to attenuate measurement noise and

1-, 2-, and 3-second previews with proportional preview gains proved to be necessary for ensuring desired dynamic performance.

Experimental setup

Engine specifications

The engine used in this investigation is a 6 L V-8 direct-injection diesel engine manufactured by the International. Its specifications are given in tab. 1. The engine is intended for a variety of medium duty truck applications covering the range between US Classes IIB and VII. Replacing the standard 6.5 L turbo charged IDI engine developing 145 kW with the more powerful International V-8 engine creates a virtual "super-Hummer" capable of providing exceptional performance even in heavier versions of the vehicle.

The engine incorporates advanced technologies to provide high power density while meeting emissions standards. A hydraulic electronic unit injector (HEUI) system permits the precise control of fuel injection timing, pressure, and quantity, and furthermore allows the use of pilot injection. An EGR circuit is used to introduce cooled exhaust gases into the intake manifold in order to decrease NO_x emissions. EGR flow rate is controlled through modulation of the EGR valve and the setting of the variable geometry turbocharger (VGT). The VGT is also used to enhance engine performance, as it reduces boost lag and allows control of the intake manifold pressure.

Table 1. Diesel engine specifications

Engine type	DI 4-stroke diesel engine
Configuration	V-8, cam-in-crankcase, 4 valves/cylinder
Bore Stroke [mm]	95 105
Displacement [L]	6.0
Rated power [kW]	250 at 3300 rpm
Rated torque [Nm]	760
Compression ratio	18.0 : 1
Valve lifters	Push rod-activated rocker arm
Aspiration	Variable geometry turbine / intercooler
Fuel delivery system	Gen. 2 hydraulic-electronic unit-injectors

Test cell systems and engine instrumentation

The engine is coupled to a 330 kW AVL ELIN series 100 APA asynchronous dynamometer. This dynamometer is especially well suited to perform transient testing, as it has a 5 ms torque response time and a –100% to +100% torque reversal time of 10 ms. Operation of the test cell is orchestrated via the AVL PUMA open system, providing an environment for monitoring and controlling test cell functions. The engine is fully instrumented for time-based measurements of pressures, temperatures, and flow rates at various locations in the system. The time-based signals are acquired with the use of AVL fast front end modules (F-FEMs). Crank angle resolved measurements include in-cylinder pressure, fuel injection pressure, and needle lift. Data acquisition and combustion analysis is performed via an AVL Indimaster Advanced 671 indicating system.

Interfacing with the engine's powertrain control module (PCM) and monitoring of control functions is accomplished through the use of ETAS INCA software. The injection parameters, as well as EGR valve and VGT vane setting, can be observed and adjusted. INCA is

linked to PUMA via a communication link that operates on the ASAM (Association for Standardization of Automation and Measuring Systems) protocol.

An AVL combustion emissions bench (CEB-II) is used to sample, condition, and measure exhaust gas constituents. Analyzers measure the proportion of carbon monoxide (CO), carbon dioxide (CO_2), oxygen (O_2), total hydrocarbons (THC), and oxides of nitrogen (NO_x) in the exhaust gas. CO_2 levels in the intake manifold are also measured to quantify EGR rates. These analyzers do not have the response time necessary to accurately follow the instantaneous temporal dynamics of emissions pulses, but they do provide an accurate integrated response [32].

Fast response emission analyzers

Accurate temporal measurement of NO_x is provided by a CLD 500 fast NO_x analyzer made by Cambustion Ltd. It consists of a chemiluminescent detector with a 90% to 10% response time of less than 3 ms for NO, and less than 10 ms for NO_x. This is achieved by locating the detectors in remote sample heads that are positioned very close to the sample point in the engine and using vacuum to convey the sample gas to the detectors through narrow heated capillaries.

The fast NO_x analyzer provides NO_x concentration in parts per million (ppm). This is subsequently converted to mass flow of NO_x with the equation:

$$\dot{m}_{NO_x} = \frac{ppm_{NO_x}}{10000} \frac{MW_{NO_x}}{MW_{exhaust}} (\dot{m}_{air} + \dot{m}_{fuel}) \tag{1}$$

where MW_{NO_x} is molecular weight of NO_x, $MW_{exhaust}$ is molecular weight of exhaust, and $(\dot{m}_{air} + \dot{m}_{fuel})$ is the total mass flow rate of exhaust.

Temporally resolved particulate concentrations are obtained using a differential mobility spectrometer (DMS) 500 manufactured by Cambustion Ltd. This instrument measures the number of particles and their spectral weighting in the 5 nm to 1000 nm size range with a time response of 200 ms. The DMS provides aerosol size spectral data by using a corona discharge to place a prescribed charge on each particle. The charged particles are then carried along a classifier column by a sheath of clean air. Within the column, particles are subjected to a radial electric field from a central electrode which repels them towards the periphery. Particles with lower aerodynamic drag-to-charge ratio will deflect more quickly and are attracted towards electrode rings closer to the beginning of the classifier column, and *vice versa*. As the particles land on the grounded rings, they give up their charge and these outputs from the electrometers are processed in real time to provide spectral data and other desired parameters.

Typical spectral data from the DMS 500 are shown in fig. 4. The x-axis is particle diameter (D_p) in nanometers and the y-axis is the spectral density with a unit of $dN/dlogD_p$ in cm^3. Thus the area under the curve represents the number of particles per cubic centimeter of sample. Conversion of aerosol spectral size data into particulate mass is not straightforward. Agglomerates formed during diesel combustion are non-spherical and therefore their mass does not correlate with the cube of the particle diameter. Similarly, the constituents of the particles change as the diameter varies and consequently there is no direct correlation between particle density and diameter. Nevertheless, a relationship has been suggested by the manufacturer [33], based on results obtained from an scanning mobility particle sizer and an aerosol particle mass spectrometer and published by Park *et al*. [34]. While these instruments use the same principles to classify particles, they require much more time (~100 s) to produce a full size spectrum.
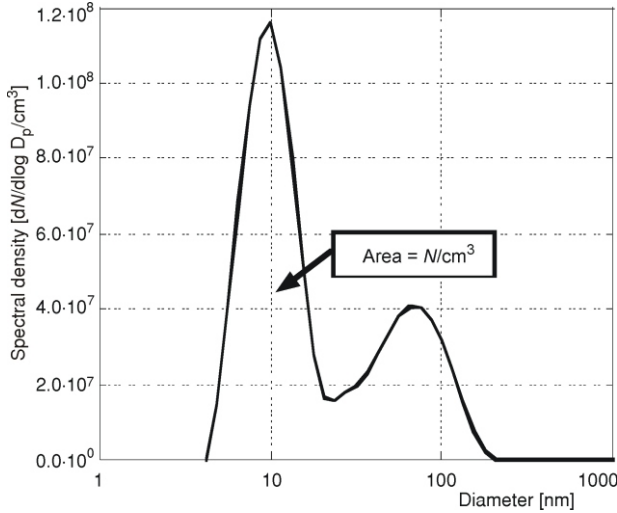
Figure 4. Sample particulate spectral density curve

To obtain total particle mass, the x-axis of the curve shown in fig. 4 is first discretized, which groups the data into particle diameter bins. The density of the particles within each bin is assumed to be constant and then the mass of particles (M_p) in each bin is determined by:

$$M_p = 6.95 \; 10^{-3} D_p^{2.34} N_p \qquad (2)$$

where N_p is the number of particles. The non-spherical nature of particle shapes is accounted for by the diameter exponent smaller than three. The leading coefficient acts as a "pseudo-density" for the particles in that bi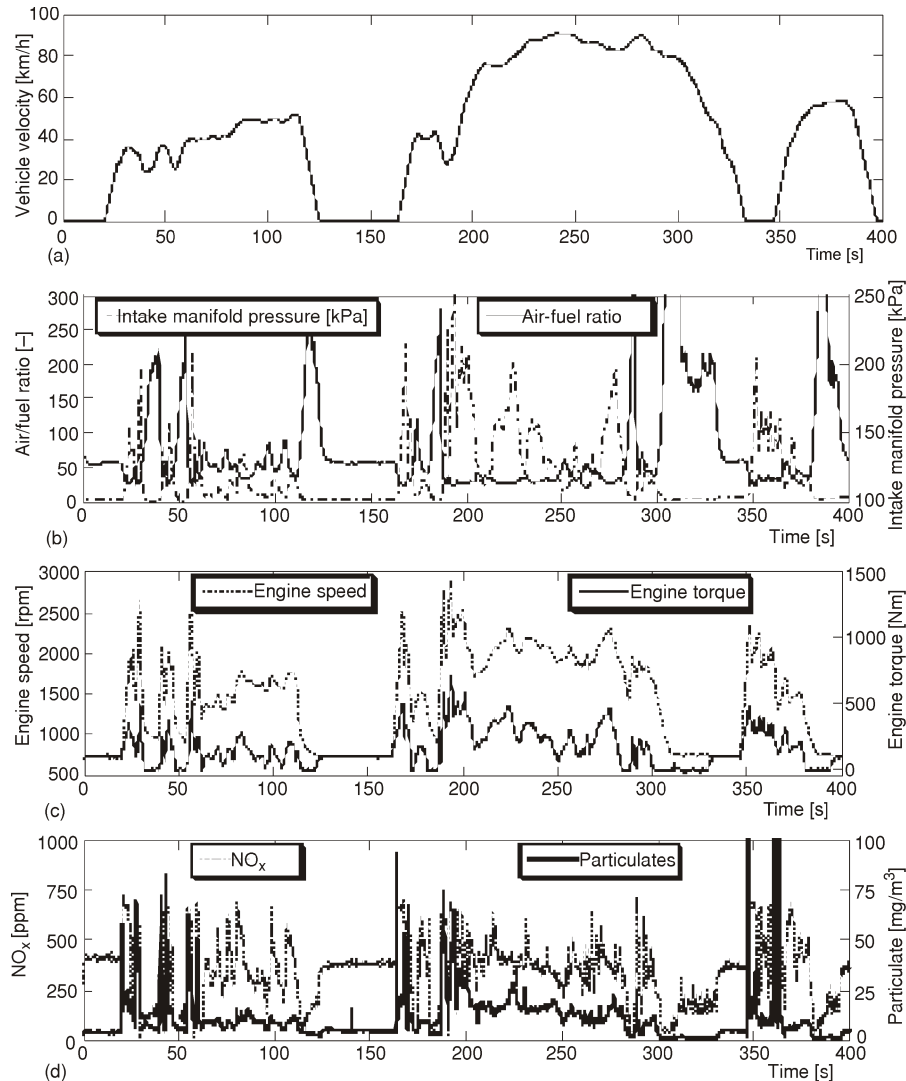n; its magnitude is affected by particle constituents and also the unit changes that occur with the non-integer particle diameter exponent. After the M_p is calculated for each bin, the total mass is found by summing the masses in each bin and dividing it by the number of bins per decade, $i.\ e.$:

$$M_T = \frac{\sum_{Bins} M_p}{Bins / Decade} [\text{kg} / \text{m}^3] \qquad (3)$$

This summation is used as an approximation that accounts for integration over a logarithmic scale.

Results – the effect of transients on diesel emissions

This section describes the drive cycle and examines interactions in the powertrain systems and dynamic responses of critical sub-systems and components. Particular attention is focused on the effect of engine system transients on exhaust emission trends and visual signature. The transient contribution to overall particulate emission is quantified, thus enabling future development of strategies for clean and efficient truck propulsion.

Typical measurements obtained over a transient driving schedule are given in fig. 5. Only the first 400 s of the Federal Urban Driving Schedule are shown rather than the whole cycle, since this interval encompasses three representative velocity profiles and allows showing data with more clarity. This schedule is commonly used for evaluating light and medium trucks.

The vehicle speed profile is shown in fig. 5(a), and this is the only input for a particular transient test run. The rest of the time-resolved profiles given in fig. 5 represent measurements obtained in the EIL facility, and thus offer insight into interactions between powertrain subsystems and components over an aggressive driving schedule. Figure 5(b) illustrates engine speed and torque profiles. The engine speed history is much more dynamic than the vehicle speed history, due to interactions with the torque converter and the transmission. The engine is idling while the vehicle is stopped. The torque profiles – see also fig. 5(b) – display even more dynamic behavior, with very sharp and frequent fluctuations between relatively low and extremely

Figure 5. Results of the EIL test over a segment of the FTP75 driving schedule
*(a) vehicle speed; (b) engine speed and torque, (c) boost pressure and air/fuel ratio, and
(d) instantaneous NO$_x$ and particulate concentration in the exhaust*

high values. It is important to note that the torque fluctuations depend not only on vehicle parameters and driving conditions, but also driver aggressiveness in correcting errors. For instance, in the process of addressing integration challenges, it was observed that the cyber-driver with shorter preview had difficulties following the schedule accurately and often behaved more aggressively, thus causing increased fluctuations of engine torque. Torque displays values higher than zero during idling since the engine has to overcome the stall losses in the torque converter.

Figure 5(c) allows going one level deeper and characterizing behavior of the turbocharging system during transient in-vehicle operation, as well as the repercussions for the in-cylinder conditions, namely the air-to-fuel (A/F) ratio. Every increase in engine command

from the driver leads to increased fueling, higher enthalpy in the exhaust and thus increased turbocharger speed. However, dynamics of the turbocharger rotor cause a lag in the response of the air-charging system, and this has a profound effect on in-cylinder processes. A closer look at fig. 5(c) reveals a gradual increase in boost pressure at the initiation of the transient due to turbo lag. This is typically accompanied with a small dip in the A/F ratio, *e. g.* around the 180 s mark or a 350 s mark. The electronic fuel injection controller obviously senses the low boost pressure value and limits the fuel; nevertheless, the instantaneous A/F values at the initiation of a transient can be somewhat below quasi-steady values observed immediately afterwards. The instantaneous NO_x and particulate emission trends are shown in fig. 5(d). The emissions profiles demonstrate a very transient behaviour, with sharp high-frequency fluctuations. Particulate concentration displays very large spikes. These spikes seem to be correlated with initiations of sudden torque increases, but while A/F ratio is obviously an important factor, fluctuations of particulate concentration are not strongly correlated with global A/F. More information is needed to fully understand the transient emissions spikes and identify additional factors affecting their magnitude.

Characterizing transient emissions

A close up of a shorter interval from a drive cycle given in fig. 6 provides more details. The instantaneous mass flow rates of particulates, derived from the fast differential mobility spectrometer measurements during the interval between 30 and 46 s, are shown in fig. 6(a). Engine command and the intake manifold pressure are plotted for the same time interval in fig. 6(b). The particulate emissions are emphasized whenever there is a sudden increase of engine load, particularly from idle.
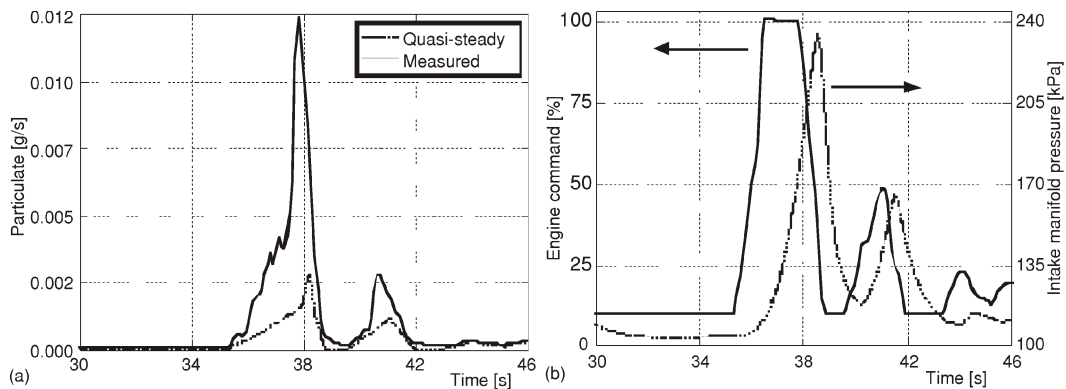

Figure 6. Engine system behaviour during a 30-46 s interval of the FTP75 vehicle driving schedule
(a) comparison of measured transient particulate mass emissions and predicted quasi-steady emissions, (b) engine command and measured intake manifold pressure

Interestingly, the sharp spike of the particulate emission does not fully align with the peak engine command. While the command often shows very rapid increases to 100%, the intake manifold pressure buildup is delayed due to turbocharger inertia, as illustrated in fig. 6(b). This is a period of irregular conditions, where the engine air supply limits the amount of fuel that can be burned. While the electronic controller monitors intake manifold pressure and its "smoke limiting" logic prevents injection of excessive amounts of fuel, the instantaneous values of A/F

ratio can still display instantaneous excursion below values observed at more steady conditions – see fig. 5(c). This will be investigated further, along with other factors likely to play a role in transient particulate emissions. Exhaust residual might still be present in the manifold even if the exhaust gas recirculation EGR valve is rapidly closed. Unfavorable pressure difference between the exhaust and intake manifold at the initiation of the load increase can lead to increased internal residual. Low boost implies reduced fresh charge velocity and poorer mixing. In summary, analysis of realistic engine operation in the vehicle indicates that transient departures have the most effect on particulate emissions, since the phasing of instantaneous particle mass (PM) spikes aligns well with the initiation of the load transient. The transient effect is most prominent when sudden load increase is initiated from idle.

Quantifying the transient effect requires establishing a reasonable baseline first. This is accomplished utilizing a simple engine model in Simulink and a map of steady-state engine particulate emission measured in the same test cell (or a "static" map). When transient speed and fueling trajectories measured in the EIL facility are provided to the Simulink engine model as input, the emission histories corresponding to assumed quasi-steady conditions are obtained as output. In other words, the quasi-steady baseline represents estimates of what the emissions would have been had we marched through the driving schedule point-by-point and allowed conditions to settle at every step. This baseline is contrasted to real instantaneous measurements obtained in the EIL facility, as shown in fig. 6(a). The spike of instantaneous particulate emission is higher and it precedes the quasi-steady predictions. The quasi-steady profile basically follows the load, its peak aligning closely with the peak in boost pressure. This confirms the hypothesis about irregular conditions at the initiation of the transient being the primary cause of transient particle emissions. The transient contribution to the total emission during the given interval is very tangible, as the integrated area under the transient trace is much greater than the area under the quasi-steady line. Consequently, the transient contribution can easily dominate the overall emission trends in case of very aggressive driving conditions for a heavy vehicle, such as those specified by the FTP75 procedure. In fact, when the cumulative particulate emissions are determined from both the transient measurements and the quasi-steady simulated trace, the results show more than doubling of the soot emission due to transients (see fig. 7). Consequently, dealing with transients has to be part of any low-emission strategy, as more than half of the total particulates can be attributed to irregular conditions initiated with rapid load increases. The dynamic aspects are also important. The large transient spikes in soot emission are linked to black smoke and they need to be addressed regardless of the total emission. In case the engine system is outfitted with the diesel particulate filter (DPF), the spikes in soot concentration will determine dynamic loading of the filter and hence be a factor in development of regeneration strategies.

Figure 7. Comparison of measured cumulative particulate emissions in grams per mile (g/mi) over a complete FTP75 driving schedule and quasi-steady emissions, estimated under the assumption of steady engine operation at each of the speed/load points
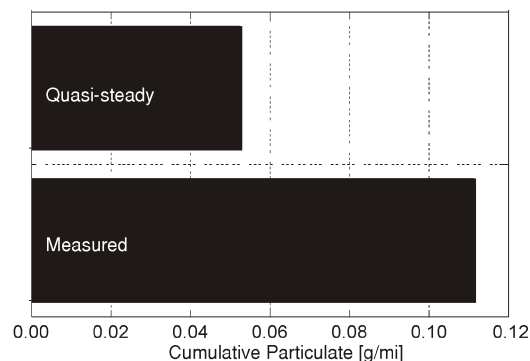
The differential mobility spectrometry provides in-depth view of the soot emission phenomena occurring during the rapid transient. Two sequences of particle size-number distributions are shown in fig. 8, with a tenth of a second resolution. The first transient increase in load illustrated in figs. 6(a) and 6(b) is captured with a sequence shown in fig. 8a. What really stands out is an extraordinary increase of soot particle size. While near-idle operation was characterized by relatively large numbers of very small particles (on average 10-15 nm in diameter), the profiles are shifted towards diameter size of 100-150 nm at the onset of a transient – note the logarithmic scale on the graph in fig. 8(a). Converting values for diameter to volume and mass magnifies the relative change; thus it is safe to say that the shift in particle size represents a puff of smoke emanating from the exhaust manifold. The features of the particulate size distributions change as the engine stabilizes somewhat at high load conditions. This is evident from the fig. 8(b), capturing the last part of the transient event. As the engine stabilizes at high boost and high fueling condition, the profiles move left and start displaying a typical dual-mode shape observed by other researchers at steady-state conditions [34]. In summary, features of particulate size-number distributions confirm the strong effect of irregular in-cylinder conditions experienced during rapid transients on soot formation. The conditions are unique, and lead to formation of very large particles, in contrast to typical dual-mode (nucleation and accumulation) profiles expected at high-load diesel operation. This is consistently seen at every initiation of the rapid load increase. The relevance of different factors influencing particulate formation will be explored further during a special tip-in test described in the next section.
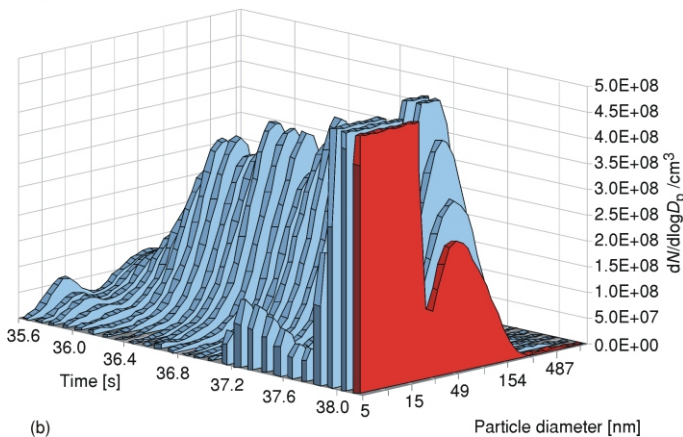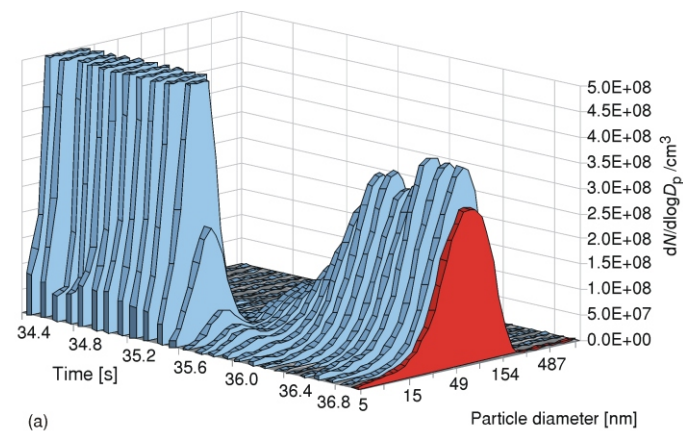

Figure 8. Sequences of particle size-number distributions obtained during a 30-46 s interval of the FTP 75 vehicle driving schedule with the differential mobility spectrometer
(a) interval capturing the beginning of the transient with a marked shift towards increased particle size at the onset of a load change
(b) interval capturing stabilization of engine operation at high load after the rapid transient, with a typical dual-mode profile

Reducing transient emissions: tip-in functions

To increase understanding of transient particulate emissions and establish guidelines for designing drive-by-wire systems and hybrid powertrain power management strategies, load tip-ins from one to nine bar break mean effective pressure (BMEP) were conducted at a constant speed of 2000 rpm. The interval over which the engine command linearly increases was varied from an instantaneous change to a five second tip-in, as illustrated in fig. 9(a). By changing the rate at which pedal position is changed, this type of experiment demonstrates the impact of driver aggressiveness and dynamic powertrain interactions on emissions. Analogously, in case the engine is used in a hybrid propulsion system, a power management strategy aggressively optimized for fuel economy might introduce frequent step-changes of engine command. Comparison of the step-change with delayed tip-in cases will yield quantification of the transient emission penalty. Establishing the tip-in features that minimize transient soot is just a first step in addressing transient emissions at the powertrain system level. Fully characterizing conditions leading to increased soot emissions will indicate most promising direction in future development of engine-level strategies, such as injection, VGT or EGR control.

Particulate emissions during the load ramp-up are shown in fig. 9(b). The instantaneous increase of engine command produces a large spike in particulate emissions at the beginning of the transient. Its peak magnitude is over ten times greater than the final steady-state value. The 2-second load ramp-up leads to a moderate hump, while the 5-second tip-in virtually eliminates any transient increase of particulates. The peak values in case of a 2- and 5-second tip-in occur closer to the end of the transient. The instantaneous load step produces 41% more particulate mass than the 5-second tip-in over the first ten seconds of the load change event. The remaining graphs, *e. g*. figs. 9(c-h), shed more light on system response and conditions responsible for transient particulate emission trends. As the transient process begins, a greater volume of fuel is injected into the cylinder to create more torque. Boost pressure, however, lags far behind, as shown in fig. 9(c), and thus the injection controller attempts to limit the fueling. A combination of boost pressure response and the injection control module (ICM) calibration logic limiting mass of fuel injected during turbo lag produces torque histories shown in fig. 9(d). In case of a step change of engine command, there is an almost instantaneous increase of torque up to 300 Nm and this indicates how much fuel can be burned at almost naturally aspirated conditions. It takes an additional second for torque to reach a target value slightly above 400 Nm, and this is dictated by the availability of air for combustion. Dynamic interactions play out quite differently in case of a 2-second tip-in, hence the target torque level is reached less than a second after the zero-second tip-in case. The fact that most of the adverse effects disappear if the tip-in is extended to only 2 s is encouraging. It indicates that a careful calibration of the tip-in function in a drive-by wire system can produce similar torque response with a significantly reduced soot penalty.

Figures 9(e) and 9(h) provide more insight into reasons for transient particulate emissions penalty. Soot emissions are normally correlated to oxygen-starved regions within the cylinder, and numerous processes contribute to more fuel-rich zones during the instantaneous load step. The fuel injection amount during the first couple of cycles after a step-change in command (0 s) overshoots above the boost-imposed limit, as indicated by the sharp spike of injection duration shown in fig. 9(e). This obviously implies an instantaneous spike of fuel-to-air ratio. Rapid increases in fuel injection pressure upon the onset of the instantaneous load step can cause spray over-penetration. The increase and overshoot of the injection pressure at ~1 s into the transient following a step-change in command is evident in fig. 9(f). At the same time, the momentum of the incoming charge and swirl intensity are reduced, and this has detrimental effect on mixing.
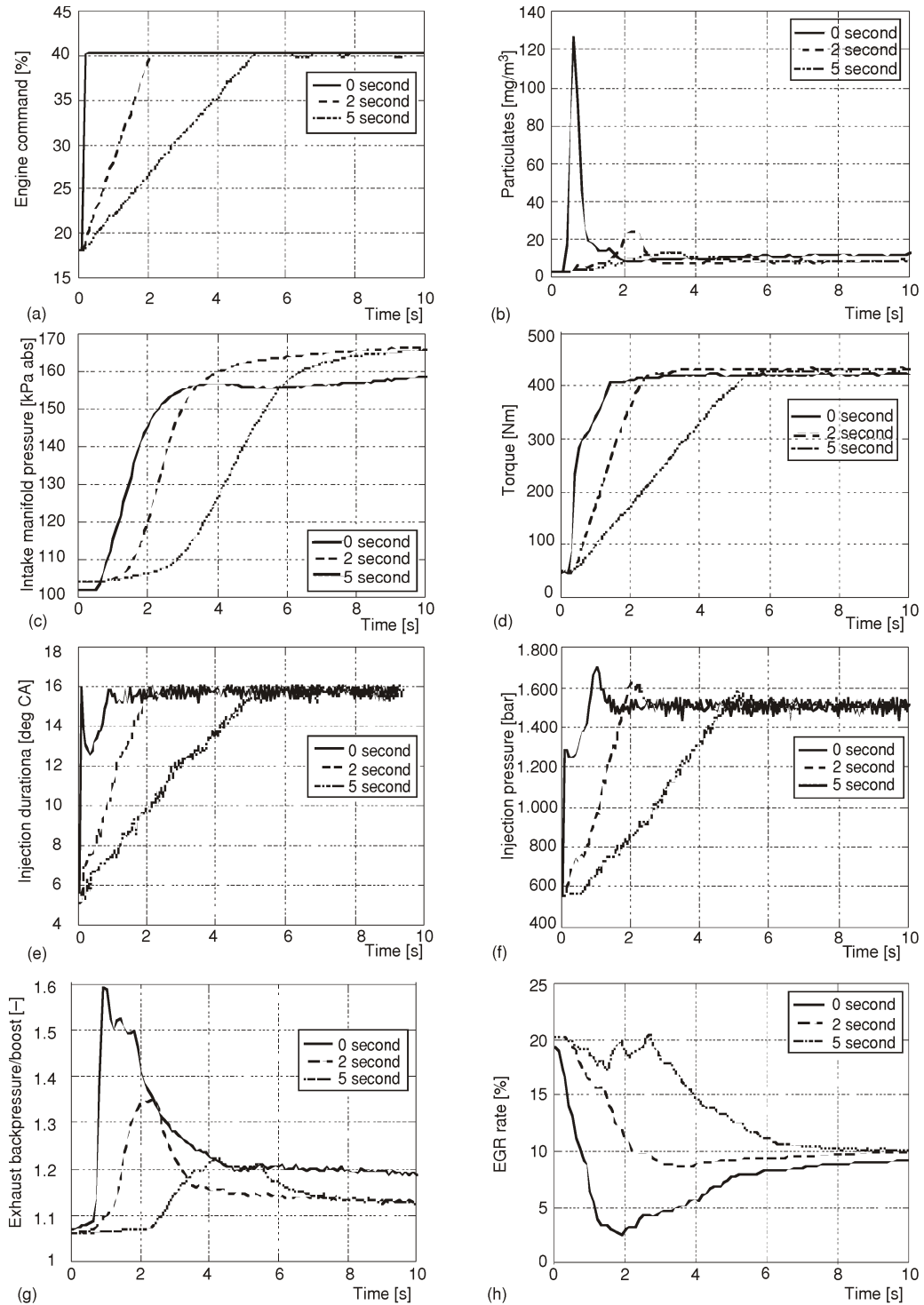
Figure 9. Analysis of engine response to varying rates of load increase
(a) tip-in functions, (b) particulate emission, (c) boost pressure, (d) torque output, (e) injection duration, (f) fuel injection pressure, (g) ratio of exhaust pressure/intake, (h) exhaust residual in the intake manifold

Finally, the ratio between the exhaust backpressure and intake manifold pressure shown in fig. 9(g) can be a significant contributing factor. High values of the p_{exh}/p_{in} ratio observed in the case of a step-change of load will cause significant increases in internal residual. Phasing of peak p_{exh}/p_{in} values correlates well with peak particulate concentration in fig. 9(b). In addition, the external (recirculated) residual is relatively high at the very beginning of the transient. The VGT settings are dynamically adjusted to reduce the target value of EGR from 20 to 10%, but the time-scales of manifold filling limit the rate at which the composition can change. Consequently, residual concentration in the intake manifold remains above the final target value during the initial couple of cycles, as shown in fig. 9(h). In summary, a combination of instantaneous overshoot of the mass of fuel injected in the cylinder, and an increased presence of residual, particularly internal, lead to significantly increased particulate formation in the initial stage of a load transient.

Relevance of findings

The EIL tests are currently the only reliable way to obtain deep insight into the effect of engine/powertrain transients on diesel emissions and hence are an essential tool in the quest for developing clean and efficient propulsion for trucks. The advanced test cell capabilities correlate engine state variables with transient emissions and offer guidance for reducing their magnitude. This enables further work on expanding this knowledge and applying it for addressing transient emissions with engine-level strategies (*e. g.* fuel injection, variable geometry turbine and/or variable valve actuation and exhaust gas recirculation strategies) or vehicle level strategies such as drive-by-wire systems, tailoring of the torque converter or transmission characteristics *etc*.

The vehicle-level analysis is particularly important in case of hybrid propulsion. On-going work by authors aims to take advantage of the EIL capabilities and examine the behavior of the engine integrated with different hybrid architectures, *e. g.* a parallel hybrid electric system or a series hydraulic hybrid system. While hybrid systems offer more flexibility in controlling the engine, optimizing the power management for fuel economy can lead to sharp load increases. Hence, follow up work will use lessons learned in the EIL facility for optimizing the trade-off between fuel economy and emissions at the vehicle level. The immersion of additional hardware, *e. g.* hydraulic pump/motors and energy storage, will expand the EIL concept to powertrain-in-the-loop studies and enable equal fidelity in evaluating transient behavior of these sub-systems and components.

Conclusions

A real medium-duty diesel engine was immersed in the virtual vehicle system to develop an EIL capability. In particular, an International 6 L V-8 DI diesel engine was integrated with a 4 4 driveline for a 5 ton off-road truck with a four-speed automatic transmission. Two critical enablers were an advanced, highly-dynamic dynamometer setup and a suite of vehicle models with appropriate fidelity. The study emphasized the use of the EIL setup as a research tool for addressing fundamental aspects of transient diesel emissions under realistic driving conditions. Hence, the EIL setup included advanced engine instrumentation for monitoring key engine processes, as well as a fast NO_x analyzer and a fast particle sizer (differential mobility spectrometer). Therefore, detailed information about interactions in the powertrain system can be correlated with transient emission trends.

The EIL setup utilizes a Matlab-Simulink interface provided by the vendor of the dynamometer and the accompanying control system. The implementation uncovered several integration challenges, such as the signal noise and stability issues, time delay in signal processing and inadequate cyber-driver response. These issues were addressed by reversing the causality of the torque converter model, the implementation of lead-lag filtering, and by introducing preview in the driver model. The engine coupled to the virtual off-road vehicle system was tested over the federal urban driving schedule. The analysis of results shows the following.

- Engine transients have very significant impact on instantaneous soot and NO_x emission. Large spikes of particulate emission are observed during initial phases of vehicle acceleration events.
- Transient particulate emissions show the largest departure from quasi-steady estimates at the initiation of a sudden load increase from idle, thus causing advanced phasing of instantaneous PM spikes. The conditions are characterized by turbo lag, *i. e.* low boost and remnants of exhaust residual from preceding steady conditions.
- A very significant increase of average particulate size is consistently seen at the initiation of rapid increases of load.
- Analysis of a transient caused by a step-change of engine command shows a sharp spike of particulate emission. The spike contributes significantly to the cumulative emission.
- While numerous processes contribute to transient particulate emission, the combination of the instantaneous overshoot of the mass of fuel injected, and an increase in internal residual (due to very high instantaneous values of the pressure ratio between exhaust and intake during turbo lag) and to a lesser extent external residual (due to time-scales of manifold filling) seem to be dominant.
- Replacing the step-increase with a two-second ramp virtually eliminates the transient effect for a 1-9 bar change of BMEP. Phase delay in torque response between a step-change and a 2 second tip-in is less than a second, since turbo lag delays engine response to a step change of load request.
- Transient effects are not visible in case of a 5-second tip-in.

Characterization of transients provides a basis for devising engine-level or vehicle level strategies. An example of the former would be multiple fuel injections or advanced intake-air and residual handling; while the latter includes drive-by-wire strategies and hybrid power management approaches. The analysis of tip-in functions can be directly utilized for development of vehicle level strategies and development of advanced hybrid propulsion systems. Virtual prototyping of the vehicle facilitates rapid changes of the propulsion system architecture and evaluation of a number of very different configurations, *e. g.* a hybrid electric power split system or a series hydraulic hybrid system.

Acknowledgment

tional Engine and Truck Corporation, and John Vanderslice and Kevin Gady from the Ford Motor Company.

References

[1] Ciesla, C. R., Jennings, M. J., A Modular Approach to Powertrain Modeling and Shift Quality Analysis, SAE paper 950419, Special publication SP-1080, 1995

[2] Assanis, D., *et. al*.,Validation and Use of Simulink Integrated, High Fidelity, Engine-In-Vehicle Simulation of the International Class VI Truck, SAE technical paper 2000-01-0288, 2000

[3] Filipi, Z., *et. al*.,Combined Optimization of Design and Power Management of the Hydraulic Hybrid Propulsion System for the 6 6 Medium Truck, *International Journal of Heavy Vehicle Systems*, *11* (2004), 3/4, pp. 371-401

[4] Filipi, Z., Wang, Y., Assanis, D.,Variable Geometry Turbine (VGT) Strategies for Improving Diesel Engine In-Vehicle Response – a Simulation Study, *International Journal of Heavy Vehicle Systems, 11* (2004), 3/4, pp. 303-326

[5] Fluga, E. C., Modeling of the Complete Vehicle Powertrain Using ENTERPRISE, SAE paper 931179, 1993

[6] Lin, C-C., *et. al*., Modeling and Control for a Medium-Duty Hybrid Electric Truck, *International Journal of Heavy Vehicle Systems, 11* (2004), 3/4, pp. 349-370

[7] Lin, C., *et. al*., Integrated, Feed-Forward Hybrid Electric Vehicle Simulation in SIMULINK and its Use for Power Management Studies, SAE technical paper 2001-01-1334, 2001

[8] Wu, B., *et. al*., Optimal Power Management for a Hydraulic Hybrid Delivery Truck, *Journal of Vehicle System Dynamics, 42* (2004), 1-2, pp. 23-40

[9] Rousseau, A., Sharer, P., Pasquier, M., Validation Process of a HEV System Analysis Model: PSAT, SAE paper 2001-01-0953, 2001

[10] Shidore, N., Pasquier, M., Interdependence of System Control and Component Sizing for a Hydrogen-Fueled Hybrid Vehicle, SAE paper 2005-01-3457, 2005

[11] Kim, H. M., *et. al*., Target Cascading in Vehicle Redesign: A Class VI Truck Study, *International Journal of Vehicle Design, 29* (2002), 3, pp. 199-225

[12] Hong, S.-Ch., Rutland, C., Reitz, R., Development of an Integrated Spray and Combustion Model for Diesel Simulations, SAE paper 2001-30-0012, 2001

[13] Hong, S., Assanis, D., Wooldridge, M., Multi-Dimensional Modeling of NO and Soot Emissions with Detailed Chemistry and Mixing in a Direct Injection Natural Gas Engine, SAE paper 2002-01-1112, 2002

[14] Nabi, S., *et. al*., An Overview of Hardware-In-the-Loop Testing Systems at Visteon, SAE paper 2004-01-1240, 2004

[15] Jason, T. C., Moskwa, J. J., A Hardware-in-the-Loop Transient Diesel Engine Test System for Control and Diagnostic Development, *Proceedings*, ASME International Mechanical Engineering Congress and Exposition, New York, USA, 2001

[16] Fleming, M., Len, G., Stryker, P., Design and Construction of a University-Based Hybrid Electric Powertrain Test Cell, SAE paper 2000-01-3106, 2000

[17] ***, Diesel Hybridization and Emissions, Argonne National Laboratory Center for Transportation Research, Report to DOE from the ANL Vehicle Systems and Fuels Team, available at http://www.osti.gov/bridge/, in paper from U.S. Department of Energy, Office of Scientific and Technical Information, P.O. Box 62, Oak Ridge, Tenn., USA, 37831-0062

[18] Louca, L. S., Yildir, U. B., Modeling and Reduction Techniques for Studies of Integrated Hybrid Vehicle Systems, *Proceedings*, 4th International Symposium on Mathematical Modeling, Vienna, Austria, 2003

[19] Louca, L., Stein, J., Rideout, D., Generating Proper Integrated Dynamic Models for Vehicle Mobility Using a Bond Graph Formulation, Society for Computer Simulation, Phoenix, Ariz., USA, 2001

[20] Sendur, P., *et. al*., A Model Accuracy and Validation Algorithm, *Proceedings,* 2002 ASME International Mechanical Engineering Congress and Exposition, New Orleans, La., USA, 2002

[21] Filipi, Z., *et. al*., Engine-in-the-Loop Testing for Evaluating Hybrid Propulsion Concepts and Transient Emissions – HMMWV Case Study, SAE paper 2006-01-0443, SAE Transactions, Journal of Commercial Vehicles, also presented 2006 SAE World Congress, Detroit, Mich., USA, 2006, pp. 23-41

[22] Kokkolaras, *et. al*., Design under Uncertainty and Assessment of Performance Reliability for a Dual-Use Medium Truck with Hydraulic-Hybrid Powertrain and Fuel Cell Auxiliary Power Unit, SAE Paper

2005-01-1396; SAE Transactions, Journal of Passenger Cars: Mechanical Systems, Warrendale, Penn., USA, 2005, pp.1651-1660

[23] Kozaki, T., *et. al*., Balancing the Speed and Fidelity of Automotive Powertrain Models Through Surrogation, *Proceedings*, ASME International Mechanical Engineering Congress and Exposition, 2004, Anaheim, Cal., USA, 2004, pp. 249-258

[24] Karnopp, D. C., Margolis, D. L., Rosenberg, R. C., System Dynamics: Modeling and Simulation of Mechatronic Systems, 3rd ed., John Wiley & Sons, New York, USA, 2000

[25] Hrovat, D., Tobler, W. F., Bond Graph Modeling and Computer Simulation of Automotive Torque Converters, *Journal of the Franklin Institute, 319* (1985), 12, pp. 93-114

[26] Louca, L. S., Stein, J. L., Energy-Based Model Reduction of Linear Systems, *Proceedings,* International Conference on Bond Graph Modeling and Simulation, San Francisco, Cal., USA, 1999

[27] Fathy, H. K., Ahlawat, R., Stein, J. L., Proper Powertrain Modeling for Engine-in-the-Loop Simulation, *Proceedings*, ASME International Mechanical Engineering Congress and Exposition, 2005, Orlando, Fl., USA, 2005, pp. 1195-1201

[28] ***, 20SIM, 20SIM Pro User's Manual. The University of Twente-Controllab Products B.V. Enschede, The Netherlands, 1999

[29] Babbit, G. R., Moskwa, J. J., Implementation Details and Test Results for a Transient Engine Dynamometer and Hardware in the Loop Vehicle Model, *Proceedings*, IEEE International Symposium on Computer-Aided Control System Design, Hawaii, USA, 1999, pp. 569-574

[30] Franklin, G. F., Powell, J. D., Emami-Naeini, A., Feedback Control of Dynamic Systems, 3rd ed., Addison-Wesley, Reading, Mass., USA, 1994

[31] Skogestad, S., Postlethwaite, I., Multivariable Feedback Control: Analysis and Design, John Wiley & Sons, New York, USA, 1997

[32] Partridge, W., *et. al*., Time-Resolved Measurements of Emission Transients by Mass Spectrometry, SAE paper 2000-01-2952; SAE Transactions, *Journal of Fuels and Lubricants, 109* (2000), pp. 2992-2999

[33] Reavell, K., Hands, T., Collings, N., A Fast-Response Particulate Spectrometer for Combustion Aerosols, SAE paper 2002-01-2714, SAE Transactions, *Journal of Fuels and Lubricants, 111* (2002), pp. 1338-1344

[34] Park, K., *et. al*., Relationship between Particle Mass and Mobility for Diesel Exhaust Particles, *Environmental Science and Technology, 37* (2003), 3, pp. 577-583

Authors' addresses:

Z. Filipi, H. Fathy
The University of Michigan,
2031 W. E. Lay Automotive Laboratory,
1231 Beal Av., Ann Arbor, MI 48109 -2133, USA

J. Hagena
PACCAR Technical Center
12479 Farm to Market Road, Mt. Vernon, WA 98273, USA

Corresponding author Z. Filipi
E-mail: filipi@umich.edu